BIOCHEMISTRY
including biophysical chemistry & molecular biology

Article

pubs.acs.org/biochemistry

Investigation of Osmolyte Effects on FolM: Comparison with Other Dihydrofolate Reductases

Purva P. Bhojane, Michael R. Duff, Jr., Harini C. Patel, Melissa E. Vogt, and Elizabeth E. Howell*

Department of Biochemistry and Cellular and Molecular Biology, University of Tennessee, Knoxville, Tennessee 37996-0840, United States

Supporting Information

ABSTRACT: A weak association between osmolytes and dihydrofolate (DHF) decreases the affinity of the substrate for the *Escherichia coli* chromosomal and R67 plasmid dihydrofolate reductase (DHFR) enzymes. To test whether the osmolyte−DHF association also interferes with binding of DHF to FolM, an *E. coli* enzyme that possesses weak DHFR activity, ligand binding was monitored in the presence of osmolytes. The affinity of FolM for DHF, measured by $k_{cat}/K_{m(DHF)}$, was decreased by the addition of an osmolyte. Additionally, binding of the antifolate drug, methotrexate, to FolM was weakened by the addition of an osmolyte. The changes in ligand binding with water activity were unique for each osmolyte, indicating preferential interaction between the osmolyte and folate and its derivatives; however, additional evidence provided support for further interactions between FolM and osmolytes. Binding of the reduced nicotinamide adenine dinucleotide phosphate (NADPH) cofactor to FolM was monitored by isothermal titration calorimetry as a control for protein−osmolyte association. In the presence of betaine (proposed to be the osmolyte most excluded from protein surfaces), the NADPH K_d decreased, consistent with dehydration effects. However, other osmolytes did not tighten binding to the cofactor. Rather, dimethyl sulfoxide (DMSO) had no effect on the NADPH K_d, while ethylene glycol and polyethylene glycol 400 weakened cofactor binding. Differential scanning calorimetry of FolM in the presence of osmolytes showed that both DMSO and ethylene glycol decreased the stability of FolM, while betaine increased the stability of the protein. These results suggest that some osmolytes can destabilize FolM by preferentially interacting with the protein. Further, these weak attractions can impede ligand binding. These various contributions have to be considered when interpreting osmotic pressure results.

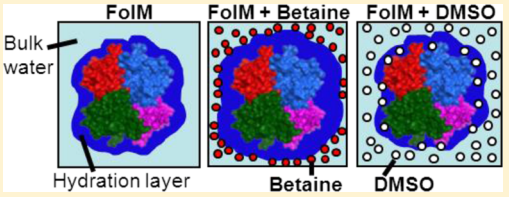

If water is involved in an interaction, perturbation of water activity will alter binding. For example, shorter contact distances usually exclude water. Typically, increasing the concentration of small molecule osmolytes results in tighter binding, consistent with dehydration of the protein−ligand interface, which leads to stronger binding as water is released.[1] We previously probed the role of water in R67 dihydrofolate reductase (DHFR) by adding various osmolytes to steady-state kinetic assays and ITC binding experiments. Tighter binding of the NADPH cofactor and weaker binding of the substrate, dihydrofolate, upon addition of the osmolyte were observed.[2] While different osmolytes had similar effects on NADPH binding, variable results were observed when DHF binding was probed.

Weaker binding of DHF in the presence of osmolytes can occur by either destabilization of the enzyme-ligand complex or stabilization of the free enzyme or the free ligand. For R67 DHFR, as each symmetry-related binding site accommodates either NADPH or DHF and different behavior is observed upon addition of the osmolyte (either weaker DHF binding or tighter cofactor binding, e.g., water release), we can use binding of NADPH to R67 as an internal control.[2−4] This analysis suggests effects on the free enzyme or the enzyme−cofactor complex are unlikely as numerous osmolytes have the same effect on cofactor binding, consistent with a preferential exclusion mechanism in which osmolytes are excluded from the protein surface.[5−8] Elimination of these options for DHF binding leaves osmolyte effects on free DHF. A corollary of the hypothesis that DHF has differential interactions with osmolytes is that related osmolyte effects should then be observed in any enzyme that uses DHF, for example, the nonhomologous chromosomal DHFR from *Escherichia coli* (EcDHFR).

Using the logic described above, osmotic stress studies were performed using EcDHFR.[9] Tighter binding of $NADP^+$ and weaker binding of DHF were again observed. The slopes associated with plots of ln $K_{a(DHF)}$, the association binding constant, versus ln(water activity) were similar for EcDHFR and R67 DHFR. Because positive slope values associated with ligand binding are unusual,[10−12] and as similar values are observed for DHF binding in two quite different DHFR scaffolds, this result supports the hypothesis that osmolytes associate weakly with free DHF. [If we consider the other side of the coin, as folate is hydrophobic with a logP value of −3.875 (logP is a partition coefficient reflecting solubility in water vs octanol), water prefers to interact with the osmolytes rather than DHF.] This model, depicted in Figure 1, uses a variation of the preferential interaction model in which the osmolytes bind DHF, albeit weakly. If osmolytes are bound and more difficult to release

Received: October 16, 2013
Revised: February 7, 2014
Published: February 11, 2014

   dx.doi.org/10.1021/bi4014165 | *Biochemistry* 2014, 53, 1330−1341

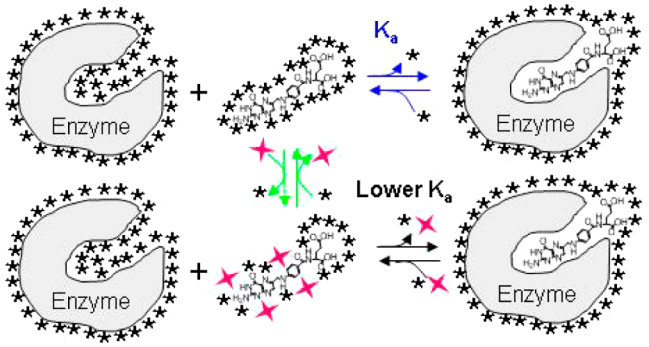

Figure 1. Model showing the preferential interaction of osmolytes with free DHF. Removal of water (★) and/or osmolytes (red symbols) from the solvation shell of DHF is required for the ligand to bind to DHFR. If the DHF−osmolyte association is stronger than the DHF−water interaction, the binding equilibrium is shifted to the left, favoring the unbound state. This results in a decreased binding affinity of DHF for DHFR. This model does not exclude interactions between osmolytes and the protein.

than water, then weaker binding of the substrate to DHFR results. In this scenario, the osmolytes shift the binding equilibrium toward the free species and inhibit complex formation.

In the next step, we question the prevalence of this phenomenon by investigating if other DHFRs continue to show the same behavior. Other enzymes capable of serving as DHFRs have been identified in organisms lacking chromosomal DHFR, also known as FolA.[13−15] For example, while pteridine reductase (PTR1) from *Leishmania major* normally reduces biopterin and dihydrobiopterin, it can also reduce DHF. The homologous gene in *E. coli* is *ydgB* (renamed *folM*). The presence of FolM allows *E. coli* to grow even when the chromosomal DHFR gene has been deleted as a double *FolA* (encoding EcDHFR) plus *FolM* deletion in *E. coli* is synthetic lethal.[16] PTR1 and FolM are short chain dehydrogenases/reductases that utilize an entirely different structure and active site residues (K198-Y194-D181 catalytic triad in PTR1).[17,18] Most recently, FolM has been proposed to be a dihydromonapterin reductase in which this substrate has a pteridine ring with a -CHOH-CHOH-CH_2OH tail.[19]

A summary of available information describing EcDHFR, R67 DHFR, PTR1, and FolM is given in Table 1.[20] Figure 2 compares the crystal structures of EcDHFR, R67 DHFR, and PTR1. While a structure and more kinetic information are available for PTR1, we chose to work with the FolM protein from *E. coli* as PTR1 shows substrate inhibition,[21] which could complicate the analysis of osmolyte effects on DHF binding.

MATERIALS AND METHODS

Protein Expression. The FolM gene from *E. coli* cloned into pET21B was a generous gift from A. Hanson (University of Florida, Gainesville, FL).[19] This FolM construct carries an N-terminal His tag (MGHHHHHHH-), and expression is controlled by a lac promoter.[13] The plasmid was transformed into Rosetta 2 *E. coli* cells (EMD Millipore). For protein expression, cells were grown at 37 °C in TB medium containing 100 μg/mL ampicillin and 30 μg/mL chloramphenicol. When the optical density reached 0.6 at 550 nm, IPTG was added to give a final concentration of 1 mM. Cells were grown for an additional 5 h, centrifuged, and frozen. For lysis, cells were resuspended in 50 mM sodium phosphate buffer (pH 8.0) containing 300 mM NaCl with 20% (v/v) glycerol and sonicated.

Table 1. Comparison of Relevant Structural and Functional Parameters for EcDHFR (pH 7.0), R67 DHFR (pH 7.0), PTR1 (pH 6.0), and FolM (pH 6.0)

	EcDHFR (FolA)	R67 DHFR (type II DHFR)	PTR1 (*L. major*)	FolM
monomer size[a]	159 amino acids, 17999 Da	78 amino acids, 8430 Da	288 amino acids, 30457 Da	240 amino acids, 27496 Da
oligomeric state	monomer[b]	tetramer[c]	tetramer[d]	tetramer (this study)
no. of active sites	1	1	4	4
structural features	eight-stranded mixed β-sheet with four α-helical connecting strands[b]	four β-barrels; single active site pore composed of residues from four subunits[c]	seven-stranded parallel β-sheet sandwiched between three α-helices on either side[d]	ND
volume of the active site[e] (Å^3)	1677 (1RA2)	3626 (1VIE)	1392−1920 (2BFA)	ND
trimethoprim K_i	20 pM[f]	150 μM[g]	ND	>1.4 mM[h]
methotrexate K_i or K_d	0.07 nM[i]	>500 μM[j]	30−255 nM[k]	5.9 μM[h]
NADPH K_m or K_d (μM)	0.94[l]	3.0[m]	14.2[k]	1.9 (K_m),[h] 3.86 ± 0.29 (K_d, this study)
DHF K_m (μM)	1.2[l]	5.8[m]	3.4[k]	9.0,[h] 4.3 ± 0.6 (this study)
k_{cat}	28 s^{-1} (product release),[l] 238 s^{-1} (hydride transfer)[n]	1.3 s^{-1}[m]	0.38 μmol min^{-1} mg^{-1} (V_{max})[k]	0.083 μmol min^{-1} mg^{-1} (V_{max}),[h] 0.240 ± 0.009 s^{-1} (k_{cat}, this study)
natural substrate	DHF	DHF	biopterin, dihydrobiopterin[k]	dihydromonapterin[o]

[a]Molecular weight calculated using http://web.expasy.org/cgi-bin/protparam/protparam. [b]From refs 76 and 77. [c]From refs 78 and 79. [d]From ref 17. [e]Calculated from Castp[80] (http://cast.engr.uic.edu/cast/). [f]From ref 81. [g]From ref 82. [h]From ref 83. [i]From ref 84. [k]The K_i value depends on substrate (from ref 21). [l]From ref 85. [m]From ref 86. [n]From ref 87. [o]From ref 19.

dx.doi.org/10.1021/bi4014165 | *Biochemistry* 2014, 53, 1330−1341

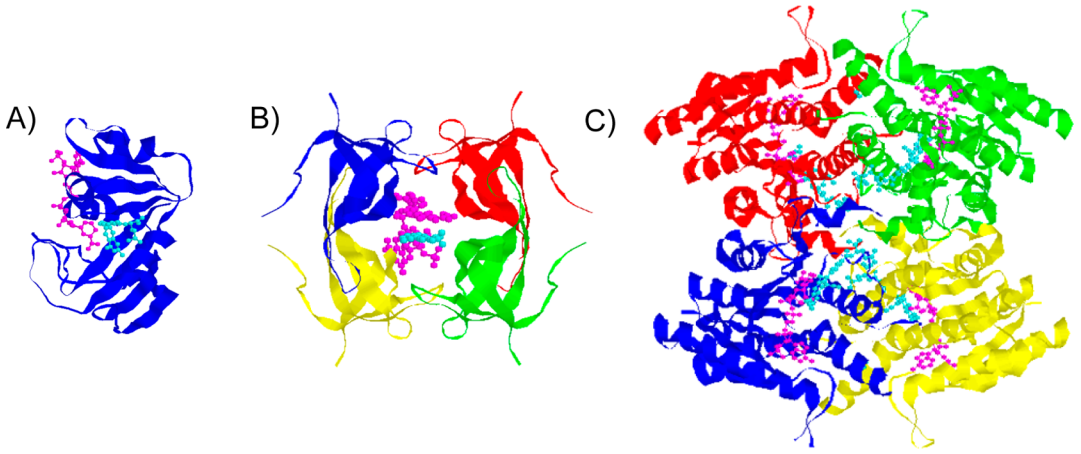

Figure 2. Structures of the various DHFRs. (A) *E. coli* chromosomal DHFR structure (PDB entry 1RA2).[88] Bound $NADP^+$ is colored magenta and bound folate cyan. (B) R67 DHFR structure (PDB entry 1VIF). Each color corresponds to a different monomer. The central doughnut hole is the active site. Bound $NADP^+$ and DHF are colored magenta and cyan, respectively.[4] (C) *L. major* PTR1 structure (PDB entry 2BFA).[18] Each different monomer is colored differently. Bound NADPH and CB3717 are colored magenta and cyan, respectively.

Purification entailed loading and elution from a Ni^{2+} nitrilotriacetic acid agarose column (Qiagen). The protein was eluted in the same buffer using a gradient from 10 to 250 mM imidazole. Sodium dodecyl sulfate−polyacrylamide gel electrophoresis analysis showed a single band, and fractions were flash-frozen in liquid N_2 and stored at −80 °C. An Econo-Pac 10DG column (Bio-Rad) was used to exchange buffers upon defrosting. Protein concentrations were determined using a bicinchoninic acid (BCA) (Pierce) assay.

Steady-State Kinetics. Steady-state kinetic data were obtained at 30 °C in MTA polybuffer at pH 6.0 using a Perkin-Elmer λ35 spectrophotometer as described previously.[22] MTA buffer consisted of 50 mM MES, 100 mM Tris, and 50 mM acetic acid; it maintains a constant ionic strength (μ = 0.1 M) from pH 4.5 to 9.5.[23] Protein concentrations in the assay were 95−280 nM. To remove a lag, the enzyme was preincubated with NADPH and the reaction initiated by addition of DHF. DHF K_m values were measured in the presence of a saturating NADPH concentration (32−76 μM). Initial rates were fit to the Michaelis−Menten equation in Sigmaplot. DHF was prepared by reduction of folate as described by Blakley.[24] NADPH was purchased from Alexis Biochemicals. Concentrations of DHF and NADPH were measured using their respective extinction coefficients at 340 nm, 7.75×10^3 and 6.23×10^3 M^{-1} cm^{-1}, respectively.[25] The extinction coefficient for the DHFR reaction is 12.3×10^3 M^{-1} cm^{-1}.[26]

Isothermal Titration Calorimetry (ITC). Affinities, stoichiometries, and enthalpies of binding were determined as previously described.[3] At least two replicate titrations were performed using a VP-ITC microcalorimeter from MicroCal; 240 s separated each injection, allowing for baseline equilibration. FolM concentrations ranged from 8.5 to 15 μM in MTA buffer (pH 6). For titrations with osmolyte present, MTA buffer and the osmolyte were used in the reference cell. The "*c* value" ($=[P_{total}]/K_d$) ranged from 1 to 8, within the suggested range of 1−1000.[27]

Origin version 7.0 was initially used to analyze the ITC data. The data were then exported into SEDPHAT; this program allows global fitting of replicate data sets.[28] A single-site model (A + B ↔ AB) was used for the fitting process, and errors were calculated using the Monte Carlo for nonlinear regression option. For some experiments, baseline slopes and noise hindered integration of the ITC data by Origin. Therefore, the automated peak analysis program NITPIC[29] was used to integrate those data files to obtain the heat for each injection before further analysis with SEDPHAT.

Ultracentrifugation. Sedimentation velocity experiments were performed using absorbance optics in a Beckman Optima XL-I ultracentrifuge. The FolM sample was exchanged into MTA buffer (pH 6), and 15.7 μM FolM monomer was used in the experiment. Sedimentation velocity analysis was conducted at 50000 rpm and 25 °C using an An50 Ti eight-hole rotor. Sedimentation velocity analysis was performed by direct boundary modeling using the Lamm equation and Sedfit[30] (see http://www.analyticalultracentrifugation.com). Partial specific volume (0.7269) and buffer viscosity values were determined using SEDNTERP[31] (see http://www.jphilo.mailway.com/download.htm). The density of the buffer was determined using an Anton Paar DMA 35 vibrating tube density meter.

Water Activity Measurements. The solution osmolality was measured using a Wescor 5500 vapor pressure osmometer. This value was converted into water activity according to the equation

$$a_{H_2O} = e^{-0.018 \times \text{osmolality}} \quad (1)$$

where a_{H_2O} is the water activity.[32]

Differential Scanning Calorimetry. Thermal unfolding of FolM was monitored between 25 and 95 °C using a Microcal VP differential scanning microcalorimeter (DSC). The instrument was operated using the data acquisition and analysis program (Origin version 7.0) supplied by the manufacturer; 9−11 μM FolM (monomer concentration) samples were prepared in MTA polybuffer (pH 6) with or without osmolytes. Scan rates were 1 and 1.5 °C/min. Scans were repeated three times.

Circular Dichroism. CD was used to monitor the effect of cosolvents on the secondary structure of FolM using an AVIV model 202 instrument. Briefly, at least five scans were taken on samples containing 9 μM protein in 50 mM phosphate buffer with 100 mM NaCl (pH 6.0) with or without the osmolyte using 0.5 nm steps and a 2 s integration. An average spectrum was calculated. The CD data were normalized as the mean residue ellipticity by using 110 g/mol as the mean residue molecular weight.[22]

dx.doi.org/10.1021/bi4014165 | *Biochemistry* 2014, 53, 1330−1341

Fluorescence Quenching. Binding of methotrexate (MTX) (Sigma-Aldrich) to 2 μM FolM was monitored in MTA buffer (pH 6) using tryptophan fluorescence as described by Zhuang et al.[33] MTX concentrations were determined at pH 13.0 using an extinction coefficient of 22000 M^{-1} cm^{-1} at 302 nm.[34] Spectra were recorded on a Perkin-Elmer LS55 fluorimeter. The sample was excited at 295 nm, and emission spectra were recorded from 315 to 450 nm. Data were fit to

$$\mathrm{Fl} = F_o - 0.5F_o\left[P_{tot} + K_d + L_{tot} - \sqrt{(P_{tot} + K_d + L_{tot})^2 - 4P_{tot}L_{tot}}\right] \quad (2)$$

where Fl is the observed fluorescence, L_{tot} is the total ligand concentration, and P_{tot}, K_d, and F_o are variables describing the number of enzyme binding sites, the dissociation constant, and the fluorescence yield per unit concentration of enzyme, respectively.

Homology Modeling. A homology model was created for FolM in MOE version 2010 (Chemical Computing Group, Montreal, QC) using the structure of *L. major* PTR1 (PDB entry 2BFA) as a template.[18] Primary sequences for FolM and PTR1 were aligned, and FolM was modeled as a tetramer. Modeling was performed using the ligands bound in the 2BFA structure (NADPH and 10-propargyl-5,8-dideazafolate) as additional templates for the active site of the protein. The homology model with the fewest deviations in the φ and ψ angles from Ramachandran values is described below.

RESULTS

Ultracentrifugation. A previous comparison of PTR1 and FolM primary sequences[13] using the ClustalW program yields a score of 22, where the score describes "the number of identities between the two sequences, divided by the length of the alignment, and represented as a percentage".[35] To determine if any homology extends past the primary sequence, the oligomerization state of FolM was assessed via sedimentation velocity analysis. The monomer mass of FolM with an N-terminal His tag is 27496.5 Da according to Expasy ProtParam[36] calculations. Figure 3 shows the ultracentrifugation data that indicate that FolM has an *s* value of 5.85 S, corresponding to a mass of 106 kDa. This mass is consistent with FolM being a tetramer, suggesting a structural homology with PTR1 beyond that of the primary sequence as PTR1 is also a tetramer.

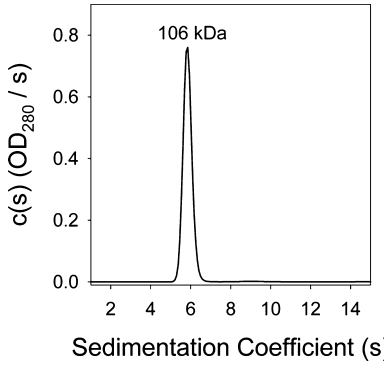

Figure 3. Sedimentation velocity data for FolM (15.7 μM) in MTA buffer (pH 6.0). The ultracentrifugation of FolM was monitored by the change in absorbance at 280 nm. The data were fit to the sedimentation distribution constant, $c(s)$, model in SedFit. A mass of 106 kDa was obtained, which indicates FolM forms a tetramer (monomer mass of 26.3 kDa). No evidence of other oligomerization states was noted.

Using this information, a homology model for FolM was constructed from the structure of tetrameric PTR1 (PDB entry 2BFA) (with bound NADPH and 10-propargyl-5,8-dideazafolate, e.g., CB3717).[17,18] Figure S1 of the Supporting Information shows this predicted structure. The predicted catalytic triad residues, D139, Y152, and K156, remain in the active site, suggesting a reasonable model. Also, R17, S87, and W89 are in the active site of the FolM homology model; the comparable residues in PTR1 interact with the dihydrobiopterin substrate in the 1E92 structure.

Stability. As our initial forays with FolM found it tended to precipitate in low-ionic strength phosphate buffer and at higher pH values, we investigated its stability using differential scanning calorimetry (DSC). Figure 4 shows the resulting thermogram.

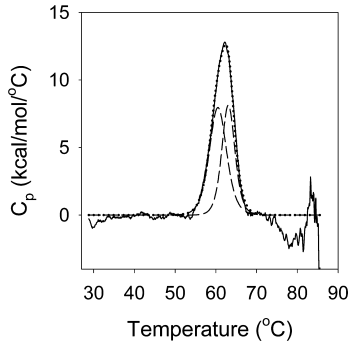

Figure 4. Fit of DSC data for FolM (11 μM) in MTA buffer (pH 6.0) at a scan rate of 1.5 °C/min. The solid black line is the DSC thermogram. The dashed black lines are fits of each of the transitions in the thermogram. The sum of the individual transition fits is shown as a dotted line that overlays the thermogram data. Fits of the data yield a T_{m1} of 60.5 ± 0.8 °C and a T_{m2} of 63.0 ± 0.3 °C.

Use of a two-state transition to fit the DSC thermogram did not accurately encompass the entire transition, so a three-state transition was used for fitting, yielding two T_m values of 60.5 ± 0.8 and 63.0 ± 0.3 °C (scan rate of 1.5 °C/min). The calorimetric enthalpy (ΔH_d) for the first transition was 42.4 ± 3.4 kcal/mol, while the ΔH_d for the second transition was 32.4 ± 3.5 kcal/mol. Thermal denaturation of FolM results in protein precipitation; thus, the scans are not reversible. Irreversible unfolding prohibited obtaining further thermodynamic information, such as the van't Hoff enthalpy.[37,38] We also considered whether FolM might display kinetic stability effects where a high free energy barrier between the native and unfolded state keeps either the unfolded or an intermediate state from aggregating.[39,40] This possibility can be tested by decreasing the scan rate.[39] As shown in Figure S2 of the Supporting Information, a slower scan rate of 1 °C/min results in lower T_m values for both transitions (58.7 ± 6.2 and 61.4 ± 1.0 °C), suggesting FolM displays kinetic stability effects.[40] Additional DSC scans were performed for a range of FolM concentrations (4−11 μM) at a scan rate of 1.5 °C/min (data not shown). Both T_m values and the ΔH_d for the first transition were constant as the protein concentration changed. The ΔH_d for the second transition increased approximately 2-fold as the FolM concentration was changed from 4 to 11 μM. The protein concentration dependence of the FolM thermogram suggests that a conformational change best describes the event

dx.doi.org/10.1021/bi4014165 | *Biochemistry* 2014, 53, 1330−1341

accompanying T_{m1}, while T_{m2} is related to tetramer dissociation. Alternatively, an increased level of aggregation of the denatured protein at higher concentrations of FolM could lead to an artificial change in T_{m2}.

Steady-State Kinetics. Previous characterization of FolM showed higher activity at lower pH.[13,19] To balance increased FolM activity with DHF solubility and NADPH stability issues, we also performed our assays at pH 6. Our steady-state kinetic values in MTA buffer are listed in Table 1. Both Giladi et al.[13] and Nare et al.[21] report V_{max} values of 0.083 μmol min^{-1} mg^{-1} for FolM and 0.38 μmol min^{-1} mg^{-1} for PTR1. While we report k_{cat} values (per FolM monomer) in Table 1, our V_{max} value (0.52 μmol min^{-1} mg^{-1}) is slightly higher than that for PTR1 (0.38 μmol min^{-1} mg^{-1}),[21] and both are higher than the value for FolM from Giladi et al. (0.083 μmol min^{-1} mg^{-1}).[13] Our DHF K_m value is also ~2-fold smaller than the value of Giladi et al.[13] These differences may arise due to variations in buffer and/or protein stability as Giladi et al.[13] used 0.1 M phosphate buffer and Pribat (personal communication)[19] found addition of 100 mM NaCl helped minimize precipitation of the protein in low-ionic strength phosphate buffer. Additionally, the crystal structure of pteridine reductase (PTR1) from *Leishmania donovani* shows sulfate occupying the phosphate binding site of the adenine-ribose phosphate for the NADPH cofactor.[41] The use of phosphate buffer by Giladi et al.[13] may provide some level of competition for cofactor binding.

Osmolyte Effects. To determine if osmolyte addition alters the secondary structure of FolM, CD scans were obtained in several osmolytes that do not absorb in the far-UV range. Figure S3 of the Supporting Information shows only minor effects, suggesting osmolyte addition does not drastically alter protein structure.

Cofactor binding was also monitored by ITC. A representative thermogram is shown in Figure S4 of the Supporting Information. Thermodynamic values for the binding of the cofactor are given in Table S1 of the Supporting Information. A linear trend between ln $K_{a(NADPH)}$ and ln(water activity) was noted for all the osmolytes used to examine cofactor binding (Figure 5). The slope of this plot indicates the preferential interaction or exclusion of the osmolytes involved in the binding of NADPH to the enzyme. The slopes associated with the individual osmolytes for this type of plot are listed in Table 2.

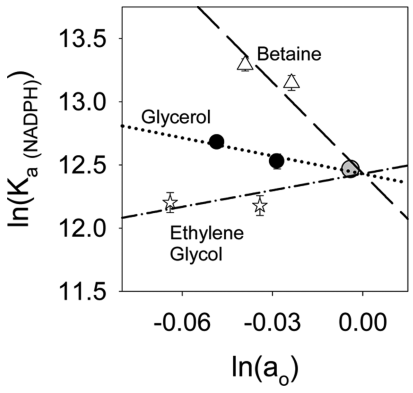

Figure 5. Effect of osmolytes, measured as water activity (a_o), on the binding of NADPH to FolM in MTA (pH 6.0). Binding was measured using ITC. The data point in buffer is shown as a gray circle, and the data for buffer and betaine (△, long dash line), glycerol (●, dotted line), and ethylene glycol (☆, dotted–dashed line) are shown. Error bars are shown and in some cases are smaller than the symbols.

As betaine has been proposed to be the osmolyte most excluded from protein surfaces,[42] it is not surprising that addition of betaine decreased the cofactor K_d (or increased the cofactor K_a). The addition of glycerol also resulted in tighter cofactor binding. In contrast, the change in $K_{d(NADPH)}$ in the presence of DMSO (10, 15, and 20%) was within error of the value for buffer alone (Figure S5A of the Supporting Information). However, cofactor binding was weakened in the presence of ethylene glycol or polyethylene glycol 400 (PEG400) (see Figure S5B of the Supporting Information for a plot of the PEG400 data). This pattern of no effect or weakened binding of cofactor in the presence of osmolytes was not noted for R67 DHFR,[2] and only sucrose decreased the level of binding of $NADP^+$ to EcDHFR,[9] suggesting a more complex behavior associated with FolM.

The thermal stability of FolM was studied to understand the weakening of cofactor binding by osmolytes. The effects of betaine, DMSO, and ethylene glycol on the thermal stability of FolM were examined by DSC (Figure 6A). Betaine increased the temperature at which FolM melted and broadened the thermogram, while DMSO decreased the melting temperature and narrowed the thermogram. The denaturation peaks still fit to two transitions. Increases of 8.8 and 9.2 °C for T_{m1} and T_{m2}, respectively, were noted in 20% betaine compared to FolM in buffer (see Figure 6B). When DMSO was considered, addition of 20% solute decreased T_{m1} by 8.5 °C and T_{m2} by 9.1 °C. Similarly, T_{m1} and T_{m2} decreased by 5.9 and 6.8 °C, respectively, in the presence of 20% ethylene glycol. The changes in T_m values were linear for betaine, ethylene glycol, and DMSO osmolality; however, opposite slopes were observed. For all three osmolytes, ΔH_d (calorimetric enthalpy of denaturation) was unchanged for the first and second thermal transitions. These results parallel other reports in the literature in which osmolytes affect the hydration shell of the protein.[43−47] When osmolytes associate with the protein surface, they are destabilizing. When osmolytes are excluded from the protein surface, they are stabilizing.

The effects of osmolytes on $k_{cat}/K_{m(DHF)}$ were investigated next. Three different osmolytes (betaine, DMSO, and sucrose) were initially chosen as they previously had significant effects on the binding of DHF to R67 DHFR and EcDHFR. These osmolytes also have different characteristics and can be used to parse out effects on viscosity and/or solution dielectric. For example, while sucrose and betaine both affect water activity, they provide opposite effects on the dielectric constant of the solution.[1,48,49] If both compounds show similar results in osmolality plots, then effects on the dielectric constant are not involved.

Using steady-state kinetics, we find addition of an osmolyte increases the $K_{m(DHF)}$ (Table S2 of the Supporting Information). Figure 7 shows the linear relationships associated with plots of ln[$k_{cat}/K_{m(DHF)}$] versus ln(water activity). As a precaution, we also plotted effects on solution viscosity or solution dielectric, and overlapping data were not observed. These figures are presented as Figures S6 and S7 of the Supporting Information. No effects on k_{cat} were noted except for ~1.5-fold increases in 20% glycerol, 20% ethylene glycol, and DMSO. In general, the slopes for FolM compare with those previously determined for R67 DHFR and EcDHFR, providing further support for our model in Figure 1. The effects of higher-molecular weight osmolytes on the binding of DHF to FolM were explored using polyethylene glycols (PEGs). Kinetic experiments using PEG400 and PEG3350 were performed with a separate FolM prep that yielded a 1.8-fold higher $k_{cat}/K_{m(DHF)}$ value in MTA buffer. PEGs have a larger effect on $k_{cat}/K_{m(DHF)}$ than small molecule osmolytes.

dx.doi.org/10.1021/bi4014165 | *Biochemistry* 2014, 53, 1330−1341

Table 2. Comparison of the Slopes of the $\ln(K_a)$ versus $\ln(a_o)$ Plots Describing the Binding of the Ligand to FolM, R67 DHFR, and EcDHFR[a]

osmolyte	$[\partial \ln(K_a)/[\partial \ln(a_o)]$ for binding of NADPH to FolM	$[\partial \ln(K_a)/[\partial \ln(a_o)]$ for binding of NADPH to R67 DHFR[c]	$[\partial \ln(K_a)/[\partial \ln(a_o)]$ for binding of NADP$^+$ to EcDHFR–DHF[d]	$[\partial \ln(K_a)/[\partial \ln(a_o)]$ for binding of DHF to FolM–NADPH[b]	$[\partial \ln(K_a)/[\partial \ln(a_o)]$ for binding of DHF to R67 DHFR–NADP$^+$[c]	$[\partial \ln(K_a)/[\partial \ln(a_o)]$ for binding of DHF to EcDHFR–NADP$^+$[d]	$[\partial \ln(K_a)/[\partial \ln(a_o)]$ for binding of MTX to FolM–NADPH
betaine	−24 ± 7	−38 ± 6	−14 ± 5	39 ± 2	60 ± 13	34 ± 9	35 ± 10
DMSO	5 ± 4	−38 ± 6	−24 ± 3	14 ± 1	41 ± 7	29 ± 1	ND[e]
sucrose	ND[e]	−38 ± 6	−5 ± 4	24 ± 4	40 ± 4	30 ± 2	ND[e]
ethylene glycol	4 ± 3	−38 ± 6	−10 ± 3	2 ± 6	25 ± 8	13 ± 1	11 ± 1
glycerol	−5 ± 1	ND[e]	−5 ± 2	−4 ± 1	16 ± 3	18 ± 1	8 ± 1
PEG400	38 ± 12	−38 ± 6	−47 ± 8	24 ± 4	78 ± 11	64 ± 5	ND[e]

[a]A negative slope is consistent with the release of water upon ligand binding, while a positive slope describes preferential binding effects that shift the equilibrium toward the unbound state. [b]Data for FolM were measured using steady-state kinetics $[k_{cat}/K_{m(DHF)}]$. [c]Data for the nonhomologous R67 DHFR were previously measured by steady-state kinetics $[k_{cat}/K_{m(DHF)}]$.[2] ITC was also used to monitor ligand binding in R67 DHFR for a subset of the osmolytes.[2] [d]Data for EcDHFR were previously measured by ITC.[9] [e]Data not determined.

As K_m can contain kinetic terms, K_d measurements would also be appropriate for testing osmolyte effects on binding. ITC measurements of binding of DHF to either apo FolM or the FolM–NADP$^+$ binary complex using ITC were unsuccessful because of a weak signal and DHF degradation over the 2–3 h duration of the titration. Therefore, we turned to binding of the antifolate methotrexate (MTX). MTX is stable at pH 6 and provides a reasonable signal. It also provides a window into osmolyte effects on folate analogues. The titration of MTX into apo FolM gave no discernible heat signal. The lack of heat released or absorbed during the titration could be due to either no binding or no signal associated with binary complex formation. To differentiate between these scenarios, the quenching of tryptophan fluorescence upon binding of MTX to FolM was measured (Figure S8 of the Supporting Information). This titration was fit to eq 2, yielding a $K_{d(MTX)}$ of 0.90 ± 0.24 μM with a stoichiometry of 0.84 ± 0.20 MTX bound per FolM monomer. Previous fluorescence studies using apo PTR1 found folate binds with a K_d of 13 μM[50] and DHF binds with a K_d of 10 μM.[21] Product inhibition studies as well as the PTR1 crystal structure indicate an ordered mechanism with cofactor binding first, followed by substrate.[17,21] For our ITC titration of MTX into FolM, the observation of no heat signal indicates entropy-driven binding. As MTX is reasonably hydrophobic (logP = −2.1654), this may be due to desolvation effects.[51]

Binding of MTX to the FolM–NADPH binary complex was also measured by ITC. A sample titration is given in Figure S9 of the Supporting Information. A K_d of 3.68 ± 0.39 μM was obtained for binding of MTX to the FolM–NADPH binary complex, which is close to the K_i of 5.9 μM determined by Giladi et al.[13] The effects of betaine, glycerol, and ethylene glycol on MTX binding were also examined (Table S3 of the Supporting Information). Compared to that with buffer alone, the $K_{d(MTX)}$ increased ∼3-fold in 20% betaine. Likewise, the $K_{d(MTX)}$ increased 1.5- and 2-fold in 20% glycerol and 20% ethylene glycol, respectively. The change in $\ln[K_{a(MTX)}]$ versus ln(water activity) of the osmolyte solutions was plotted (Figure 8). Slopes for the betaine, ethylene glycol, and glycerol data in these plots were 35 ± 10, 11 ± 1, and 8 ± 1, respectively. To the best of our knowledge, this is the first examination of osmolyte effects on MTX binding, and the results parallel the FolM DHF binding effects listed in Table 2. We note similar positive slopes were previously obtained for binding of DHF to the R67 DHFR–NADP$^+$ and EcDHFR–NADP$^+$ complexes in betaine and glycerol (Table 2).[2,9]

To analyze the binding mechanism further,[52] a 1:1 mixture of NADPH and MTX was titrated into FolM. The data could be fit to a single-binding site model. The enthalpy obtained was −22.1 ± 0.1 kcal/mol, which is close to the sum of the enthalpies for the binding of NADPH to apo FolM and binding of MTX to the NADPH–FolM binary complex (−25 kcal/mol). Similarly, the ΔG for the concurrent titration of both ligands was −15.5 ± 0.1 kcal/mol, while the sum of the ΔG values for the NADPH binary and MTX ternary titrations was −14.8 kcal/mol. The near equivalence of the ΔG and ΔH values for the titration of MTX and NADPH into FolM with the sum of the NADPH binary and MTX ternary experiments, coupled with no enthalpy associated with MTX binary binding, is consistent with an ordered binding mechanism in which NADPH binds first, followed by MTX.[52] Two alternate possibilities are that MTX binds first and rearranges upon NADPH binding or that the cofactor binding site is not totally

dx.doi.org/10.1021/bi4014165 | Biochemistry 2014, 53, 1330–1341

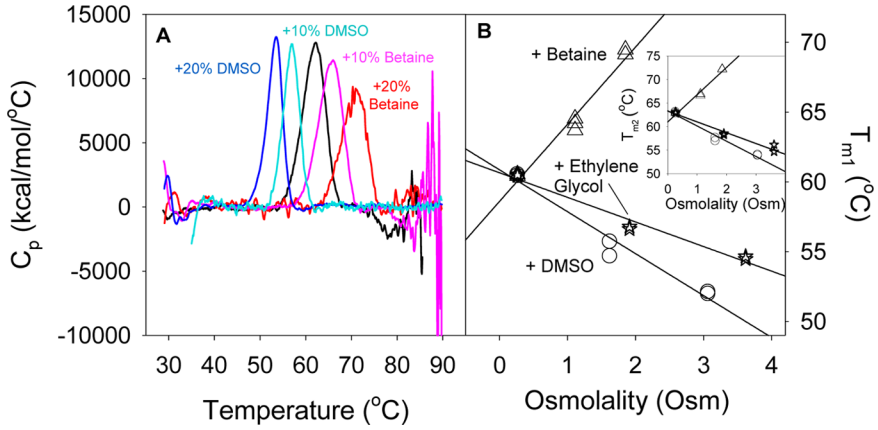

Figure 6. (A) Effect of osmolytes on the thermal stability of FolM in MTA buffer (pH 6.0) (black line), buffer with 10% betaine (magenta), buffer with 20% betaine (red), buffer with 10% DMSO (cyan), and buffer with 20% DMSO (blue). All DSC experiments were performed with a scan rate of 1.5 °C/min. (B) Effect of betaine (△), DMSO (○), and ethylene glycol (☆) on T_{m1} of FolM in MTA buffer (pH 6.0). The effects of betaine, DMSO, and ethylene glycol on T_{m2} are shown in the inset.

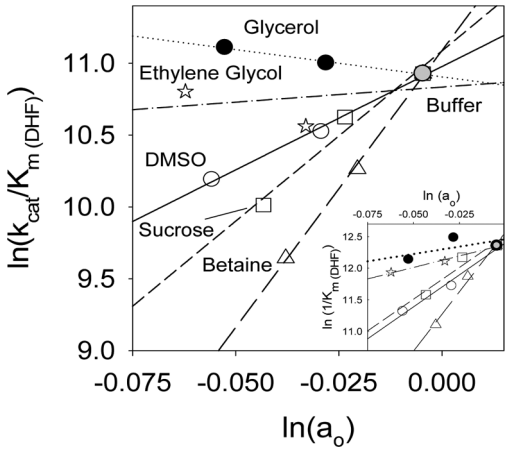

Figure 7. Effect of osmolytes on the DHF reduction activity of FolM in MTA buffer (pH 6.0). Activity studies were performed in the presence of buffer (gray circle), betaine (△), DMSO (○), sucrose (□), glycerol (●), and ethylene glycol (☆). The change in $1/K_{m(DHF)}$ with water activity (a_o) is shown in the inset. Slopes of the plots are listed in Table 2.

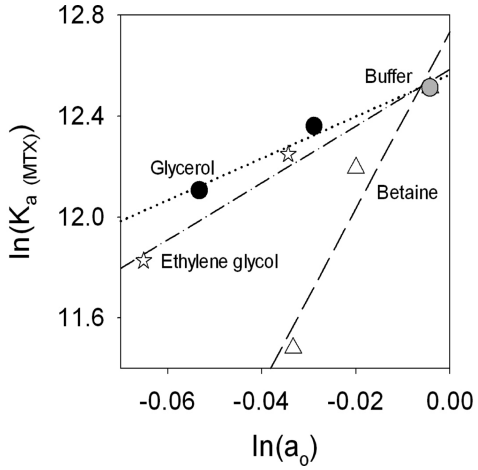

Figure 8. Effect of osmolytes, measured as water activity (a_o), on binding of MTX to the FolM−NADPH complex in MTA (pH 6.0) at 25 °C. ITC studies were performed in buffer (gray circle), betaine (△), ethylene glycol (☆), and glycerol (●).

occluded so that the cofactor can bind without release of MTX. Luba et al. found nonproductive binding of DHF to PTR1, extending the similarities between FolM and PTR1.[53]

DISCUSSION

One model of how enzymes work considers desolvation.[54−59] As cosolutes can compete with water to associate with molecular surfaces, we now expand the desolvation model of enzyme action to include removal of cosolutes such as osmolytes. If the DHF−osmolyte pairs are more difficult to break than the DHF−H_2O pairs (desolvation), then weaker binding of the substrate to DHFR results. This is a solvent substitution scenario, and as shown in Figure 1, this situation shifts the binding equilibrium toward the free species.

Because our model posits the critical species for the osmolyte effects is the DHF substrate rather than the DHFR enzyme, we ask whether our observation can be extended to other DHFRs (and ultimately to other folate utilizing enzymes). To test this model, we have previously used R67 DHFR and EcDHFR; we now add FolM to the list. We chose FolM as a representative short chain dehydrogenase that can reduce DHF. While FolM has not been as well characterized as the canonical pteridine reductase, PTR1, it does not show substrate inhibition.

Previous characterization of the FolM protein has been minimal. In this study, we provide several additional details. Our ultracentrifugation studies find FolM is a tetramer. This observation is consistent with the structure of the canonical pteridine reductase, PTR1, which is also tetrameric.[17] A FolM homology model produced using PDB entry 2BFA for PTR1[18] leads to a FolM model with the proposed catalytic triad residues placed in the active site cavity. Nearby the FolM active site are residues R237 and R168, which appear to be close enough to form ion pairs with the α- and γ-carboxylates of the Glu tail of DHF and provide tighter binding than the proposed dihydromonapterin substrate.[19] [For comparison, the Nε atom of R287 is 3 Å from the α-carboxylate of bound CB3717 (antifolate) in the active site of PTR1 in PDB entry 2BFA.] Another pertinent observation is that binding of DHF to FolM has a weak enthalpic signal, making binding difficult to measure by ITC.

Binding of the antifolate methotrexate to FolM was also characterized. To garner additional information about the binding mechanism, SEDPHAT was used to globally fit both binary

dx.doi.org/10.1021/bi4014165 | Biochemistry 2014, 53, 1330−1341

complex titrations as well as the ternary complex.[28] Figure S10 of the Supporting Information shows the global fit, and Table S4 of the Supporting Information gives the fit values. In general, the global fit values are similar to those derived from the individual fits. Binding thermodynamics obtained from the global fit indicated that MTX binds to apo FolM, with a minimal ΔH of 0.81 kcal/mol. (Fit values are not appreciably altered when ΔH is set to 0 kcal/mol, though the errors are large.) The ΔG for binding (−8.12 kcal/mol, K_d of 1.09 μM) was surprisingly more negative than that for either the NADPH binary or MTX ternary experiments. This fit value concurs with the fluorescence quenching data for binding of MTX to apo FolM, indicating tighter MTX binary than ternary binding. The difference between binding of MTX to apo FolM and the FolM−NADPH binary complex suggests that MTX may bind somewhat differently depending upon whether NADPH is already bound. This is not surprising because, in PTR1, NADPH forms part of the MTX binding site.[17,18] While FolM has many other interesting features, we chose to pursue osmolyte effects.

Betaine Effects on Ligand Binding. As DHFR uses two substrates, an internal control monitors the effects of osmolytes on binding of the second ligand and/or cofactor. This allows us to determine if osmolytes associate with folate by observation of weaker folate binding in the presence of osmolytes coupled with tighter binding of the second ligand. In the presence of betaine, NADPH binds more tightly to FolM, while DHF binds more weakly. A decrease in $K_{d(NADPH)}$ with an increasing betaine concentration is consistent with preferential exclusion of betaine from FolM and/or NADPH. Similar trends of betaine on cofactor and substrate binding were noted for both R67 DHFR and EcDHFR.[2,9] These results continue to support our model in Figure 1 in which betaine associates with free DHF. They also support more general models in which betaine acts as a natural protective molecule in *E. coli* under times of osmotic stress and is the osmolyte most excluded from protein surfaces.[42,60−63] A related observation is that betaine typically increases the stability of proteins by an increased hydration mechanism.[64,65]

Betaine also weakens the binding of methotrexate. As MTX differs from folate by the substitution of an amine group for a carbonyl off C4 of the pterin ring as well as a methyl group off N10, these changes apparently do not greatly alter the weak attraction with betaine. Our previous nuclear magnetic resonance and osmometry results found betaine weakly associates with both the pterin and benzoyl rings of folate.[66] Also, Capp et al.[62] has studied the interaction of betaine with small molecules and found that betaine associates with aromatic groups and amide nitrogens. Both these moieties are found in DHF as well as MTX; thus, it is not surprising that betaine effects on MTX binding are also found. This analysis suggests that preferential interaction with osmolytes is likely a general property of folate derivatives. It also predicts that *in vivo* binding of antifolates will be weakened by osmotic stress conditions.

The interaction between betaine and other molecules can be predicted using μ_{23}/RT values established by the Record group.[62] μ_{23}/RT values, closely related to preferential interaction coefficients, measure the favorability of a molecule (in this case, betaine) interacting with another solute as compared to water. From Table 1 of ref 62, the strongest association exists between betaine and sodium benzoate (μ_{23}/RT value of −0.091 m^{-1}). A negative (repulsive) interaction was found between betaine and tripotassium citrate with a μ_{23}/RT value of 1.2 m^{-1}. Intermediate μ_{23}/RT values span this range and allow prediction of interaction potentials, from strong to weak. NADPH has a predicted μ_{23}/RT value of 1.11 m^{-1}, indicating that its interactions with betaine are unfavorable. From the data in Figure 5, a $\Delta\mu_{23}/RT$ of 0.43 ± 0.13 m^{-1} was calculated for the interaction of betaine with NADPH. This is slightly lower than the predicted value, but it still predicts minimal association between betaine and NADPH. Our results for binding of the cofactor to FolM, as well as R67 DHFR[2] and EcDHFR,[9] indicate negative interactions between betaine and NADPH, concurring with the predicted μ_{23}/RT value. Likewise, the predicted μ_{23}/RT values for DHF, folate, and MTX (0.35, −0.01, and 0.01, respectively) indicate they are more likely to associate with betaine; this calculation agrees qualitatively with our experimental results. The $\Delta\mu_{23}/RT$ values calculated from Figures 7 and 8 are −0.69 ± 0.03 and −0.63 ± 0.17 m^{-1} for DHF and MTX, respectively. While the experimental values are different from the predicted μ_{23}/RT values, the presence of other solutes in the experiment may potentially affect the actual $\Delta\mu_{23}/RT$ value. Overall, this analysis suggests exclusion of betaine from the solvation shell of NADPH and preferential interaction of betaine with folate, DHF, and MTX.

Other Osmolytes Weaken Ligand Binding. In contrast to betaine, other osmolytes weaken the binding of NADPH to FolM. It is unlikely that these osmolytes are attracted to NADPH, as DMSO, ethylene glycol, and PEG400 all increased the affinity of the cofactor for R67 DHFR and EcDHFR.[2,9] The most likely alternative is that these osmolytes associate with FolM.[8,67] This is an additional complicating factor.

For most osmolytes studied, the $k_{cat}/K_{m(DHF)}$ decreased with added osmolyte, with most of the effects on $K_{m(DHF)}$. These results are similar to the decrease in $k_{cat}/K_{m(DHF)}$ for R67 DHFR with increasing osmolyte concentrations.[2] The most likely cause of the decrease in the FolM $k_{cat}/K_{m(DHF)}$ is association of the osmolyte with free DHF. The range in slopes for $k_{cat}/K_{m(DHF)}$ with water activity indicates that there are differences in the preferential interaction between glycerol or betaine (for example) and DHF and/or that there are additional attractions between the osmolytes and FolM.[42,67] Similar preferential interactions were also noted for binding of DHF to EcDHFR.[9] In addition, binding of the antifolate drug methotrexate was monitored and found to be weakened by the addition of osmolytes.

How Do Osmolytes Alter Ligand Binding? There are several options for how osmolytes affect the binding of both cofactor and substrate to FolM. Osmolyte effects on NADPH affinity for R67 DHFR and EcDHFR were mostly due to changes in water activity by the osmolytes.[2,9] However, in the FolM case, some osmolytes increase the affinity of NADPH, while others decrease the affinity. One scenario that could account for these variable effects is one in which some osmolytes may bind to FolM in such a way as to prevent NADPH from binding. This could involve osmolyte binding and/or solvation of FolM in the active site. Alternatively, osmolyte association at another site(s) could alter the conformation of FolM or the population of apo FolM states such that the cofactor binding equilibrium is shifted toward the free state.[68,69] Removal of these osmolytes would require input of energy to the system and lead to weaker binding of NADPH to FolM.

While osmolytes that are excluded from the protein surface stabilize proteins (e.g., trimethylamine oxide with chemically modified RNase T_1,[70] FolM with betaine), denaturants that interact with the protein (for example, urea) destabilize proteins.[70−74]

dx.doi.org/10.1021/bi4014165 | *Biochemistry* 2014, 53, 1330−1341

DMSO,[44,45] as well as other osmolytes,[43] has also been found to destabilize proteins. Lin and Timasheff propose it is the difference between association of the cosolvent with the native and denatured state that affects the stability of a protein compared to water.[75] From this point of view, while the interactions of DMSO or ethylene glycol with FolM are not so apparent upon comparison of the CD spectra with and without osmolytes, these weak interactions are clear when NADPH K_d values and T_m values are compared. While addition of DMSO and ethylene glycol did not weaken the binding of the cofactor to R67 DHFR and EcDHFR, apparently the different sequence, surface, and/or structure of FolM results in an attractive effect. Thus, each protein presents different contexts and effects. The case with betaine (most excluded) allows evaluation of the simplest case, while addition of other osmolytes can have variable effects that depend on the protein.

Once sufficient NADPH is added to overcome the negative effect of the osmolyte−FolM interaction, work has been done. It is not clear whether other osmolyte−FolM interactions are present and also exact a penalty on binding of DHF or MTX to the FolM−NADPH complex. Again, the clearest case involves betaine, where the two effects are more clearly separated. Preferential exclusion of betaine from NADPH and FolM results in water release upon NADPH binding (tighter K_d values). However, association of betaine with DHF or MTX results in weaker substrate and/or inhibitor binding. Occam's razor suggests this pattern will continue with the other osmolytes with the added layer of osmolyte−FolM effects. When the slope values are compared for the $\ln[k_{cat}/K_{m(DHF)}]$ versus $\ln(a_o)$ plots, if osmolyte−FolM interactions affected DHF binding (in addition to osmolyte−DHF interactions), we might expect even larger positive numbers. However, the values are generally smaller than those observed for R67 DHFR and EcDHFR. This observation may suggest osmolyte−FolM effects do not further weaken DHF ternary complex formation.

Another consideration that may come into play with respect to the smaller positive slopes (Table 2) associated with the FolM $\ln[k_{cat}/K_{m(DHF)}]$ versus $\ln(a_o)$ plot is the contact area between DHF and the FolM−NADPH complex. Based on the crystal structure of PTR1 with the folate-based inhibitor CB3717,[18] portions of the pterin and PABA rings do not contact the binding site; instead, they are exposed to solution. Similarly, parts of the substrate may also be solvent-exposed when bound to FolM. In this scenario, the number of osmolytes that have to be removed from DHF prior to its binding to FolM may be less than for R67 DHFR or EcDHFR because of this difference in solvent exposure. With fewer osmolytes removed, the increase in FolM $K_{m(DHF)}$ or $K_{d(MTX)}$ would not be as great as it is for R67 DHFR or EcDHFR.

Comparison of DHFR Enzymes. Osmolytes influence the binding of ligands to FolM differently compared to that for R67 DHFR and EcDHFR. For both R67 DHFR and EcDHFR, each osmolyte had a unique effect on DHF binding.[2,9] These results are interpreted as the preferential interaction of the osmolytes with the proteins.[42,67] Different slopes were noted for binding of DHF to FolM, as well (Figure 7), which suggests preferential interaction of the osmolytes with FolM. However, unlike the other DHFRs, FolM binding of NADPH is also weakened in the presence of some osmolytes (Figure 5). The destabilizing interactions of osmolytes with FolM also perturb cofactor binding.

Though R67 DHFR, EcDHFR, and FolM all have DHFR activity, they all have very different structures (Figure 2). All three have weakened substrate binding in the presence of osmolytes, indicating that interactions of the osmolyte with free DHF do shift the substrate binding equilibrium toward the free state. However, the three DHFR enzymes all interact to different extents with the osmolytes, as well. The different sequence and structural characteristics of each enzyme make each enzyme more, or less, susceptible to associating with osmolytes. In the case of FolM, some of these osmolyte interactions can destabilize the enzyme, weakening ligand binding, as well. Unfortunately, a comparison of the active sites of R67 DHFR, EcDHFR, FolM, and two pteridine reductases does not show large differences in character, precluding prediction of protein−osmolyte effects at this time. More details of the comparison are provided in the Supporting Information.

CONCLUSION

Preferential interaction of osmolytes with DHF and the antifolate methotrexate decreases their affinity for FolM. In addition to the interaction of osmolytes with the substrate and/or inhibitor, some osmolytes associate with and destabilize FolM. Destabilization of FolM by DMSO, ethylene glycol, and PEG400 weakens the binding affinity of NADPH. These osmolyte−FolM interactions may also contribute to the decrease in DHF affinity. Therefore, while interaction between osmolytes and DHF can be noted for FolM, additional interactions between some osmolytes with FolM complicate the analysis.

ASSOCIATED CONTENT

Supporting Information

A table of the thermodynamic values for the binding of NADPH to FolM, a table of the kinetic parameters for reduction of DHF by FolM, a table of the binding data for the binding of methotrexate to the FolM−NADPH complex, a table describing global fit values for binary and ternary ITC titrations, the homology model structure of FolM based on the 2BFA crystal structure of PTR1, DSC thermograms showing the effect of scan rate on the T_m of FolM, a plot of the effect of osmolytes on the CD spectra of the FolM secondary structure, a representative ITC thermogram and fit of data for the binding of NADPH to FolM, a plot of $\ln[K_{a(NADPH)}]$ in the presence of DMSO and PEG400, a plot of the change in $\ln[k_{cat}/K_{m(DHF)}]$ versus solution viscosity, a plot of the change in $\ln[k_{cat}/K_{m(DHF)}]$ versus dielectric constant, a fluorescence quenching titration of MTX into apo FolM, a representative ITC thermogram and fit of data for the binding of methotrexate to FolM, a global fit of six ITC titrations describing binary and ternary complex formation, and a discussion of the different character of the DHFR and PTR1 active sites as well as a figure showing a multiple-sequence alignment of FolM and PTR1 characterized by a disorder prediction site. This material is available free of charge via the Internet at http://pubs.acs.org.

AUTHOR INFORMATION

Corresponding Author

*Department of Biochemistry, Cell and Molecular Biology, University of Tennessee, Knoxville, TN 37996-0840. E-mail: lzh@utk.edu. Phone: (865) 974-4507. Fax: (865) 974-6306.

Funding

This work was supported by National Science Foundation Grant MCB-0817827 and internal funds from the University of Tennessee.

Notes

The authors declare no competing financial interest.

■ ACKNOWLEDGMENTS

We thank Ed Wright for running the ultracentrifugation samples. We thank Anne Pribat for her many helpful comments on her previous FolM experiments. We thank Jerome Baudry and Hong Guo for their help with the homology modeling of FolM. We thank Ms. M. Katie Kelley for her help with initial cofactor binding experiments.

■ ABBREVIATIONS

CB3717, 10-propargyl-5,8-dideazafolate; DHF, dihydrofolate; DSC, differential scanning calorimetry; ΔH_d, calorimetric enthalpy; EcDHFR, chromosomal dihydrofolate reductase from *E. coli*; ITC, isothermal titration calorimetry; MTA buffer, 100 mM Tris, 50 mM MES, and 50 mM acetate buffer; MTX, methotrexate; $NADP^+$ and NADPH, oxidized and reduced nicotinamide adenine dinucleotide phosphate, respectively; PDB, Protein Data Bank; PTR1, pteridine reductase; R67 DHFR, R67 dihydrofolate reductase.

■ REFERENCES

(1) Fried, M. G., Stickle, D. F., Smirnakis, K. V., Adams, C., MacDonald, D., and Lu, P. (2002) Role of hydration in the binding of lac repressor to DNA. *J. Biol. Chem. 277*, 50676−50682.

(2) Chopra, S., Dooling, R., Horner, C. G., and Howell, E. E. (2008) A balancing act: Net uptake of water during dihydrofolate binding and net release of water upon NADPH binding in R67 dihydrofolate reductase. *J. Biol. Chem. 283*, 4690−4698.

(3) Bradrick, T. D., Beechem, J. M., and Howell, E. E. (1996) Unusual binding stoichiometries and cooperativity are observed during binary and ternary complex formation in the single active pore of R67 dihydrofolate reductase, a D_2 symmetric protein. *Biochemistry 35*, 11414−11424.

(4) Krahn, J., Jackson, M., DeRose, E. F., Howell, E. E., and London, R. E. (2007) Structure of a type II dihydrofolate reductase ternary complex: Use of identical binding sites for unrelated ligands. *Biochemistry 46*, 14878−14888.

(5) Arakawa, T., and Timasheff, S. N. (1985) The stabilization of proteins by osmolytes. *Biophys. J. 47*, 411−414.

(6) Timasheff, S. N. (1993) The control of protein stability and association by weak interactions with water: How do solvents affect these processes? *Annu. Rev. Biophys. Biomol. Struct. 22*, 67−97.

(7) Street, T. O., Bolen, D. W., and Rose, G. D. (2006) A molecular mechanism for osmolyte-induced protein stability. *Proc. Natl. Acad. Sci. U.S.A. 103*, 13997−14002.

(8) Parsegian, V. A., Rand, R. P., and Rau, D. C. (2000) Osmotic stress, crowding, preferential hydration, and binding: A comparison of perspectives. *Proc. Natl. Acad. Sci. U.S.A. 97*, 3987−3992.

(9) Grubbs, J., Rahmanian, S., DeLuca, A., Padmashali, C., Jackson, M., Duff, M. R., Jr., and Howell, E. E. (2011) Thermodynamics and solvent effects on substrate and cofactor binding in *Escherichia coli* chromosomal dihydrofolate reductase. *Biochemistry 50*, 3673−3685.

(10) Dzingeleski, G. D., and Wolfenden, R. (1993) Hypersensitivity of an enzyme reaction to solvent water. *Biochemistry 32*, 9143−9147.

(11) Furukawa, Y., and Morishima, I. (2001) The role of water molecules in the association of cytochrome P450cam with putidaredoxin. An osmotic pressure study. *J. Biol. Chem. 276*, 12983−12990.

(12) Xavier, K. A., Shick, K. A., Smith-Gil, S. J., and Willson, R. C. (1997) Involvement of water molecules in the association of monoclonal antibody HyHEL-5 with bobwhite quail lysozyme. *Biophys. J. 73*, 2116−2125.

(13) Giladi, M., Altman-Price, N., Levin, I., Levy, L., and Mevarech, M. (2003) FolM, a new chromosomally encoded dihydrofolate reductase in *Escherichia coli*. *J. Bacteriol. 185*, 7015−7018.

(14) Levin, I., Mevarech, M., and Palfey, B. A. (2007) Characterization of a novel bifunctional dihydropteroate synthase/dihydropteroate reductase enzyme from *Helicobacter pylori*. *J. Bacteriol. 189*, 4062−4069.

(15) Myllykallio, H., Leduc, D., Filee, J., and Liebl, U. (2003) Life without dihydrofolate reductase FolA. *Trends Microbiol. 11*, 220−223.

(16) Levin, I., Giladi, M., Altman-Price, N., Ortenberg, R., and Mevarech, M. (2004) An alternative pathway for reduced folate biosynthesis in bacteria and halophilic archaea. *Mol. Microbiol. 54*, 1307−1318.

(17) Gourley, D. G., Schuttelkopf, A. W., Leonard, G. A., Luba, J., Hardy, L. W., Beverley, S. M., and Hunter, W. N. (2001) Pteridine reductase mechanism correlates pterin metabolism with drug resistance in trypanosomatid parasites. *Nat. Struct. Biol. 8*, 521−525.

(18) Schuttelkopf, A. W., Hardy, L. W., Beverley, S. M., and Hunter, W. N. (2005) Structures of *Leishmania major* pteridine reductase complexes reveal the active site features important for ligand binding and to guide inhibitor design. *J. Mol. Biol. 352*, 105−116.

(19) Pribat, A., Blaby, I. K., Lara-Nunez, A., Gregory, J. F., III, de Crecy-Lagard, V., and Hanson, A. D. (2010) FolX and FolM are essential for tetrahydromonapterin synthesis in *Escherichia coli* and *Pseudomonas aeruginosa*. *J. Bacteriol. 192*, 475−482.

(20) Yahashiri, A. (2010) Comparative investigations of H-transfer in dihydrofolate reductases from different families. Ph.D. Thesis, University of Iowa, Iowa City, IA.

(21) Nare, B., Hardy, L. W., and Beverley, S. M. (1997) The roles of pteridine reductase 1 and dihydrofolate reductase-thymidylate synthase in pteridine metabolism in the protozoan parasite *Leishmania major*. *J. Biol. Chem. 272*, 13883−13891.

(22) Strader, M. B., Smiley, R. D., Stinnett, L. G., VerBerkmoes, N. C., and Howell, E. E. (2001) Role of S65, Q67, I68, and Y69 residues in homotetrameric R67 dihydrofolate reductase. *Biochemistry 40*, 11344−11352.

(23) Ellis, K. J., and Morrison, J. F. (1982) Buffers of constant ionic strength for studying pH-dependent processes. *Methods Enzymol. 87*, 405−426.

(24) Blakley, R. L. (1960) Crystalline dihydropteroylglutamic acid. *Nature 188*, 231−232.

(25) Horecker, B. L., and Kornberg, A. (1948) The extinction coefficients of the reduced band of pyridine nucleotides. *J. Biol. Chem. 175*, 385−390.

(26) Baccanari, D., Phillips, A., Smith, S., Sinski, D., and Burchall, J. (1975) Purification and properties of *Escherichia coli* dihydrofolate reductase. *Biochemistry 14*, 5267−5273.

(27) Wiseman, T., Williston, S., Brandts, J. F., and Lin, L. N. (1989) Rapid measurement of binding constants and heats of binding using a new titration calorimeter. *Anal. Biochem. 179*, 131−137.

(28) Houtman, J. C., Brown, P. H., Bowden, B., Yamaguchi, H., Appella, E., Samelson, L. E., and Schuck, P. (2007) Studying multisite binary and ternary protein interactions by global analysis of isothermal titration calorimetry data in SEDPHAT: Application to adaptor protein complexes in cell signaling. *Protein Sci. 16*, 30−42.

(29) Keller, S., Vargas, C., Zhao, H., Piszczek, G., Brautigam, C. A., and Schuck, P. (2012) High-precision isothermal titration calorimetry with automated peak-shape analysis. *Anal. Chem. 84*, 5066−5073.

(30) Schuck, P. (2000) Size-distribution analysis of macromolecules by sedimentation velocity ultracentrifugation and Lamm equation modeling. *Biophys. J. 78*, 1606−1619.

(31) Laue, T. M., Shah, B. D., Ridgeway, T. M., and Pelletier, S. L. (1992) in *Analytical Ultracentrifugation in Biochemistry and Polymer Science* (Harding, S. E., Rowe, A. J., and Horton, J. C., Eds.) pp 90−125, Royal Society of Chemistry, Cambridge, U.K.

(32) Sweeney, T. E., and Beuchat, C. A. (1993) Limitations of methods of osmometry: Measuring the osmolality of biological fluids. *Am. J. Physiol. 264*, R469−R480.

(33) Zhuang, P., Yin, M., Holland, J. C., Peterson, C. B., and Howell, E. E. (1993) Artificial duplication of the R67 dihydrofolate reductase gene to create protein asymmetry: Effects on protein activity and folding. *J. Biol. Chem. 268*, 22672−22679.
(34) Seeger, D. R., Cosulich, D. B., Smith, J. M., Jr., and Hultquist, M. E. (1949) Analogs of pteroylglutamic acid. III. 4-Amino derivatives. *J. Am. Chem. Soc. 71*, 1753−1758.
(35) Larkin, M. A., Blackshields, G., Brown, N. P., Chenna, R., McGettigan, P. A., McWilliam, H., Valentin, F., Wallace, I. M., Wilm, A., Lopez, R., Thompson, J. D., Gibson, T. J., and Higgins, D. G. (2007) Clustal W and Clustal X versions 2.0. *Bioinformatics 23*, 2947−2948. http://www.ebi.ac.uk/Tools/msa/clustalw2/help/faq.html#21 (accessed May 2012).
(36) Artimo, P., Jonnalagedda, M., Arnold, K., Baratin, D., Csardi, G., de Castro, E., Duvaud, S., Flegel, V., Fortier, A., Gasteiger, E., Grosdidier, A., Hernandez, C., Ioannidis, V., Kuznetsov, D., Liechti, R., Moretti, S., Mostaguir, K., Redaschi, N., Rossier, G., Xenarios, I., and Stockinger, H. (2012) ExPASy: SIB Bioinformations Resource Portal. *Nucleic Acids Res. 40*, W597−W603. http://web.expasy.org/protparam/ (accessed May 2012).
(37) Sturtevant, J. M. (1987) Biochemical applications of differential scanning calorimetry. *Annu. Rev. Phys. Chem. 38*, 463−488.
(38) Johnson, C. M. (2013) Differential scanning calorimetry as a tool for protein folding and stability. *Arch. Biochem. Biophys. 531*, 100−109.
(39) Sanchez-Ruiz, J. M., Lopez-Lacomba, J. L., Cortijo, M., and Mateo, P. L. (1988) Differential scanning calorimetry of the irreversible thermal denaturation of thermolysin. *Biochemistry 27*, 1648−1652.
(40) Sanchez-Ruiz, J. M. (2010) Protein kinetic stability. *Biophys. Chem. 148*, 1−15.
(41) Barrack, K. L., Tulloch, L. B., Burke, L. A., Fyfe, P. K., and Hunter, W. N. (2011) Structure of recombinant *Leishmania donovani* pteridine reductase reveals a disordered active site. *Acta Crystallogr. F67*, 33−37.
(42) Courtenay, E. S., Capp, M. W., Anderson, C. F., and Record, M. T., Jr. (2000) Vapor pressure osmometry studies of osmolyte-protein interactions: Implications for the action of osmoprotectants in vivo and for the interpretation of "osmotic stress" experiments in vitro. *Biochemistry 39*, 4455−4471.
(43) Singh, L. R., Poddar, N. K., Dar, T. A., Kumar, R., and Ahmad, F. (2011) Protein and DNA destabilization by osmolytes: The other side of the coin. *Life Sci. 88*, 117−125.
(44) Torreggiani, A., Di Foggia, M., Manco, I., De Maio, A., Markarian, S. A., and Bonora, S. (2008) Effect of sulfoxides on the thermal denaturation of hen lysozyme: A calorimetric and Raman study. *J. Mol. Struct. 891*, 115−122.
(45) Yang, Z. W., Tendian, S. W., Carson, W. M., Brouillette, W. J., Delucas, L. J., and Brouillette, C. G. (2004) Dimethyl sulfoxide at 2.5% (v/v) alters the structural cooperativity and unfolding mechanism of dimeric bacterial NAD^+ synthetase. *Protein Sci. 13*, 830−841.
(46) Mitra, L., Smolin, N., Ravindra, R., Royer, C., and Winter, R. (2006) Pressure perturbation calorimetric studies of the solvation properties and the thermal unfolding of proteins in solution: Experiments and theoretical interpretation. *Phys. Chem. Chem. Phys. 8*, 1249−1265.
(47) Attri, P., Venkatesu, P., and Lee, M. J. (2010) Influence of osmolytes and denaturants on the structure and enzyme activity of α-chymotrypsin. *J. Phys. Chem. B 114*, 1471−1478.
(48) Edsall, J. (1943) Dielectric constants and dipole moments of dipolar ions. In *Proteins, Amino Acids and Peptides as Ions and Dipolar Ions* (Cohn, E., and Edsall, J., Eds.) pp 140−154, Reinhold, New York.
(49) Kiser, J. R., Monk, R. W., Smalls, R. L., and Petty, J. T. (2005) Hydration changes in the association of Hoechst 33258 with DNA. *Biochemistry 44*, 16988−16997.
(50) Chang, C.-F., Bray, T., and Whiteley, J. M. (1999) Mutant PTR1 proteins from *Leishmania tarentolae*: Comparative kinetic properties and active-site labeling. *Arch. Biochem. Biophys. 368*, 161−171.
(51) Kawasaki, Y., and Freire, E. (2011) Finding a better path to drug selectivity. *Drug Discovery Today 16*, 985−990.
(52) Perozzo, R., Jelesarov, I., Bosshard, H. R., Folkers, G., and Scapozza, L. (2000) Compulsory order of substrate binding to herpes simplex virus type 1 thymidine kinase. A calorimetric study. *J. Biol. Chem. 275*, 16139−16145.
(53) Luba, J., Nare, B., Liang, P. H., Anderson, K. S., Beverley, S. M., and Hardy, L. W. (1998) *Leishmania major* pteridine reductase 1 belongs to the short chain dehydrogenase family: Stereochemical and kinetic evidence. *Biochemistry 37*, 4093−4104.
(54) Lewis, C. A., Jr., and Wolfenden, R. (2009) Orotic acid decarboxylation in water and nonpolar solvents: A potential role for desolvation in the action of OMP decarboxylase. *Biochemistry 48*, 8738−8745.
(55) Wolfenden, R. (1983) Waterlogged molecules. *Science 222*, 1087−1093.
(56) Cannon, W. R., and Benkovic, S. J. (1998) Solvation, reorganization energy, and biological catalysis. *J. Biol. Chem. 273*, 26257−26260.
(57) Warshel, A., Aqvist, J., and Creighton, S. (1989) Enzymes work by solvation substitution rather than by desolvation. *Proc. Natl. Acad. Sci. U.S.A. 86*, 5820−5824.
(58) Levy, Y., and Onuchic, J. N. (2006) Water mediation in protein folding and molecular recognition. *Annu. Rev. Biophys. Biomol. Struct. 35*, 389−415.
(59) Dewar, M. J., and Storch, D. M. (1985) Alternative view of enzyme reactions. *Proc. Natl. Acad. Sci. U.S.A. 82*, 2225−2229.
(60) Cayley, S., Lewis, B. A., Guttman, H. J., and Record, M. T., Jr. (1991) Characterization of the cytoplasm of *Escherichia coli* K-12 as a function of external osmolarity. Implications for protein-DNA interactions in vivo. *J. Mol. Biol. 222*, 281−300.
(61) Cayley, S., and Record, M. T., Jr. (2003) Roles of cytoplasmic osmolytes, water, and crowding in the response of *Escherichia coli* to osmotic stress: Biophysical basis of osmoprotection by glycine betaine. *Biochemistry 42*, 12596−12609.
(62) Capp, M. W., Pegram, L. M., Saecker, R. M., Kratz, M., Riccardi, D., Wendorff, T., Cannon, J. G., and Record, M. T., Jr. (2009) Interactions of the osmolyte glycine betaine with molecular surfaces in water: Thermodynamics, structural interpretation, and prediction of m-values. *Biochemistry 48*, 10372−10379.
(63) Guinn, E. J., Pegram, L. M., Capp, M. W., Pollock, M. N., and Record, M. T., Jr. (2011) Quantifying why urea is a protein denaturant, whereas glycine betaine is a protein stabilizer. *Proc. Natl. Acad. Sci. U.S.A. 108*, 16932−16937.
(64) Santoro, M. M., Liu, Y., Khan, S. M., Hou, L. X., and Bolen, D. W. (1992) Increased thermal stability of proteins in the presence of naturally occurring osmolytes. *Biochemistry 31*, 5278−5283.
(65) Felitsky, D. J., and Record, M. T., Jr. (2004) Application of the local-bulk partitioning and competitive binding models to interpret preferential interactions of glycine betaine and urea with protein surface. *Biochemistry 43*, 9276−9288.
(66) Duff, M. R., Jr., Grubbs, J., Serpersu, E., and Howell, E. E. (2012) Weak interactions between folate and osmolytes in solution. *Biochemistry 51*, 2309−2318.
(67) Timasheff, S. N. (2002) Protein-solvent preferential interactions, protein hydration, and the modulation of biochemical reactions by solvent components. *Proc. Natl. Acad. Sci. U.S.A. 99*, 9721−9726.
(68) Boehr, D. D., and Wright, P. E. (2008) How do proteins interact? *Science 320*, 1429−1430.
(69) Kumar, S., Ma, B., Tsai, C.-J., Sinha, N., and Nussinov, R. (2000) Folding and binding cascades: Dynamic landscapes and population shifts. *Protein Sci. 9*, 10−19.
(70) Baskakov, I. V., Kumar, R., Srinivasan, G., Ji, Y. S., Bolen, D. W., and Thompson, E. B. (1999) Trimethylamine N-oxide-induced cooperative folding of an intrinsically unfolded transcription-activating fragment of human glucocorticoid receptor. *J. Biol. Chem. 274*, 10693−10696.

(71) Diamant, S., Eliahu, N., Rosenthal, D., and Goloubinoff, P. (2001) Chemical chaperones regulate molecular chaperones in vitro and in cells under combined salt and heat stresses. *J. Biol. Chem. 276*, 39586−39591.
(72) Venkatesu, P., Lee, M. J., and Lin, H. M. (2009) Osmolyte counteracts urea-induced denaturation of α-chymotrypsin. *J. Phys. Chem. B 113*, 5327−5338.
(73) Wu, P., and Bolen, D. W. (2006) Osmolyte-induced protein folding free energy changes. *Proteins 63*, 290−296.
(74) Belluzo, S., Boeris, V., Farruggia, B., and Pico, G. (2011) Influence of stabilizers cosolutes on catalase conformation. *Int. J. Biol. Macromol. 49*, 936−941.
(75) Lin, T. Y., and Timasheff, S. N. (1994) Why do some organisms use a urea-methylamine mixture as osmolyte: Thermodynamic compensation of urea and trimethylamine N-oxide interactions with protein. *Biochemistry 33*, 12695−12701.
(76) Bolin, J., Filman, D., Matthews, D., Hamlin, R., and Kraut, J. (1982) Crystal structures of *Escherichia coli* and *Lactobacillus casei* dihydrofolate reductase refined at 1.7 Å resolution. I. General features and binding of methotrexate. *J. Biol. Chem. 257*, 13650.
(77) Filman, D. J., Bolin, J. T., Matthews, D. A., and Kraut, J. (1982) Crystal structures of *Escherichia coli* and *Lactobacillus casei* dihydrofolate reductase refined at 1.7 Å resolution. II. Environment of bound NADPH and implications for catalysis. *J. Biol. Chem. 257*, 13663−13672.
(78) Matthews, D. A., Smith, S. L., Baccanari, D. P., Burchall, J. J., Oatley, S. J., and Kraut, J. (1986) Crystal structure of a novel trimethoprim-resistant dihydrofolate reductase specified in *Escherichia coli* by R-plasmid R67. *Biochemistry 25*, 4194−4204.
(79) Narayana, N., Matthews, D. A., Howell, E. E., and Nguyen-huu, X. (1995) A plasmid-encoded dihydrofolate reductase from trimethoprim-resistant bacteria has a novel D_2-symmetric active site. *Nat. Struct. Biol. 2*, 1018−1025.
(80) Liang, J., Edelsbrunner, H., and Woodward, C. (1998) Anatomy of protein pockets and cavities: Measurement of binding site geometry and implications for ligand design. *Protein Sci. 7*, 1884−1897.
(81) Stone, S. R., and Morrison, J. F. (1986) Mechanism of inhibition of dihydrofolate reductases from bacterial and vertebrate sources by various classes of folate analogues. *Biochim. Biophys. Acta 869*, 275−285.
(82) Amyes, S. G., and Smith, J. T. (1976) The purification and properties of the trimethoprim-resistant dihydrofolate reductase mediated by the R-factor, R388. *Eur. J. Biochem. 61*, 597−603.
(83) Howell, E. E., Villafranca, J. E., Warren, M. S., Oatley, S. J., and Kraut, J. (1986) Functional role of aspartic acid-27 in dihydrofolate reductase revealed by mutagenesis. *Science 231*, 1123−1128.
(84) Jackson, M., Chopra, S., Smiley, R. D., Maynord, P. O., Rosowsky, A., London, R. E., Levy, L., Kalman, T. I., and Howell, E. E. (2005) Calorimetric studies of ligand binding in R67 dihydrofolate reductase. *Biochemistry 44*, 12420−12433.
(85) Howell, E. E., Booth, C., Farnum, M., Kraut, J., and Warren, M. S. (1990) A second-site mutation at phenylalanine-137 that increases catalytic efficiency in the mutant aspartate-27 → serine *Escherichia coli* dihydrofolate reductase. *Biochemistry 29*, 8561−8569.
(86) Reece, L. J., Nichols, R., Ogden, R. C., and Howell, E. E. (1991) Construction of a synthetic gene for an R-plasmid-encoded dihydrofolate reductase and studies on the role of the N-terminus in the protein. *Biochemistry 30*, 10895−10904.
(87) Dion, A., Linn, C. E., Bradrick, T. D., Georghiou, S., and Howell, E. E. (1993) How do mutations at phenylalanine-153 and isoleucine-155 partially suppress the effects of the aspartate-27 → serine mutation in *Escherichia coli* dihydrofolate reductase? *Biochemistry 32*, 3479−3487.
(88) Sawaya, M. R., and Kraut, J. (1997) Loop and subdomain movements in the mechanism of *Escherichia coli* dihydrofolate reductase: Crystallographic evidence. *Biochemistry 36*, 586−603.